Title

Bacterial cytological profiling rapidly identifies the cellular pathways targeted by antibacterial molecules

Journal

Proceedings of the National Academy of Sciences of the United States of America, 110(40)

ISSN

0027-8424

Authors

Nonejuie, Poochit
Burkart, Michael
Pogliano, Kit
et al.

Publication Date

2013-10-01

DOI

10.1073/pnas.1311066110

Peer reviewed

Bacterial cytological profiling rapidly identifies the cellular pathways targeted by antibacterial molecules

Poochit Nonejuie[a], Michael Burkart[b], Kit Pogliano[a], and Joe Pogliano[a,1]

[a]Division of Biological Sciences, University of California, San Diego, CA 92093; and [b]Department of Chemistry and Biochemistry, University of California, San Diego, CA 92093

Edited by Christopher T. Walsh, Harvard Medical School, Boston, MA, and approved August 22, 2013 (received for review June 10, 2013)

Identifying the mechanism of action for antibacterial compounds is essential for understanding how bacteria interact with one another and with other cell types and for antibiotic discovery efforts, but determining a compound's mechanism of action remains a serious challenge that limits both basic research and antibacterial discovery programs. Here, we show that bacterial cytological profiling (BCP) is a rapid and powerful approach for identifying the cellular pathway affected by antibacterial molecules. BCP can distinguish between inhibitors that affect different cellular pathways as well as different targets within the same pathway. We use BCP to demonstrate that spirohexenolide A, a spirotetronate that is active against methicillin-resistant *Staphylococcus aureus,* rapidly collapses the proton motive force. BCP offers a simple, one-step assay that can be broadly applied, solving the longstanding problem of how to rapidly determine the cellular target of thousands of compounds.

antibiotic resistance | drug screening | pharmacology | susceptibility | high throughput

Bacteria grow in complex communities where they are constantly exposed to molecules secreted by neighboring cells. Molecules that kill bacteria or strongly inhibit their growth are important evolutionary forces that determine the outcomes of bacterial interactions with each other and with host immune defenses (1–5). For example, secreted antibacterial compounds contribute to the overall composition and organization of complex microbial communities (5) while a variety of antimicrobial compounds produced by the innate immune system help to keep pathogens at bay (6). Identifying antimicrobial molecules and their cellular targets is essential for understanding how bacteria interact with one another and with other cell types (5). Knowledge of a molecule's mode of action is also important for understanding how these molecules evolve, as well as the mechanisms by which resistance can arise (7, 8). Due to the extensive use of antibiotics in the clinic, pathogenic bacteria have evolved resistance to nearly every known class of antibiotic, creating an urgent need for molecules with unique mechanisms (8, 9). Although it is relatively easy to identify molecules with antibacterial properties, determining their mechanism of action (MOA) is a notoriously difficult task that is essential for advancing hits through the discovery pipeline (8). Traditionally, a variety of assays are performed to determine whether one of five basic pathways is inhibited. These efforts typically begin with macromolecular synthesis (MMS) assays that use radioactively labeled precursors to determine whether a compound specifically inhibits protein, RNA, DNA, lipid, or peptidoglycan synthesis or whether it blocks all simultaneously (10). Although MMS is widely used throughout the pharmaceutical discovery community, it has several drawbacks. First, compounds that rapidly kill cells, such as bleach and nisin, are grouped within the sixth category of "all hitter," even though they have different mechanisms of action. Second, it can identify only a very small fraction of the total number of potential mechanisms of action. Third, in most cases, MMS assays cannot distinguish between inhibitors that effect different steps of the same pathway. Finally, MMS assays are relatively slow. Therefore, MMS assays suffer from low resolution, low accuracy, and relatively low throughput.

To overcome the shortcomings inherent in MMS assays, several alternative methods for determining MOA have been developed (8), including isolating resistant mutants, transcriptional profiling, using a collection of strains that are sensitized to hundreds of pathways, or using species with different resistance properties (11–17). Each of these approaches is complementary to each other and has unique advantages. The genetic approach is often able to identify the molecular target of an antibiotic, the specific amino acid residues important for its interaction and the frequency with which resistance occurs. The sensitized and resistant strain methods can also identify specific cellular targets, providing much higher resolution than MMS. Transcriptional profiling offers the advantages of providing insights into the pathways that are inhibited as well as the physiological responses to antibiotic stress.

Despite many advantages, these approaches also have drawbacks that have limited their utility. The genetic approach and transcriptional profiling are relatively slow and for many antibiotics fail to correctly identify the molecular target. The sensitized and resistant-strain methods suffer from requiring a large number of specialized strains to be assayed at various concentrations of antibiotic. These methods also require substantial amounts of purified compound, yet newly isolated lead compounds are often available in very small quantities. Thus, to date, there is no single, simple assay to rapidly and accurately determine the MOA for a newly isolated compound. Here, we demonstrate that bacterial cytological profiling (BCP) can discriminate between antibacterial compounds with different MOA and accurately predict the MOA of newly isolated compounds, an approach similar to cytological profiling of eukaryotic cells (18, 19). We previously used fluorescence microscopy to discriminate between compounds that have different effects on the bacterial cell envelope (20). Here, we more broadly apply BCP to a library of antibacterial compounds that target many of the clinically relevant pathways in Gram-negative bacteria and to a molecule with an unknown MOA (Table S1).

Significance

Some bacteria have evolved resistance to nearly every known class of antibiotic, creating an urgent need for new ones that work by different mechanisms. However, there has been no simple way to determine how new antibiotics work. We have developed a unique method that provides a shortcut for understanding how antibiotics kill bacteria. This method can be used to sift through compounds to rapidly identify and characterize antibiotics that work against multidrug-resistant pathogens.

Author contributions: P.N., K.P., and J.P. designed research; P.N. performed research; M.B. contributed new reagents/analytic tools; P.N., K.P., and J.P. analyzed data; and P.N., K.P., and J.P. wrote the paper.

Conflict of interest statement: J.P. and K.P. own stock in Linnaeus Bioscience Inc.

This article is a PNAS Direct Submission.

[1]To whom correspondence should be addressed. E-mail: jpogliano@ucsd.edu.

This article contains supporting information online at www.pnas.org/lookup/suppl/doi:10.1073/pnas.1311066110/-/DCSupplemental.

MICROBIOLOGY

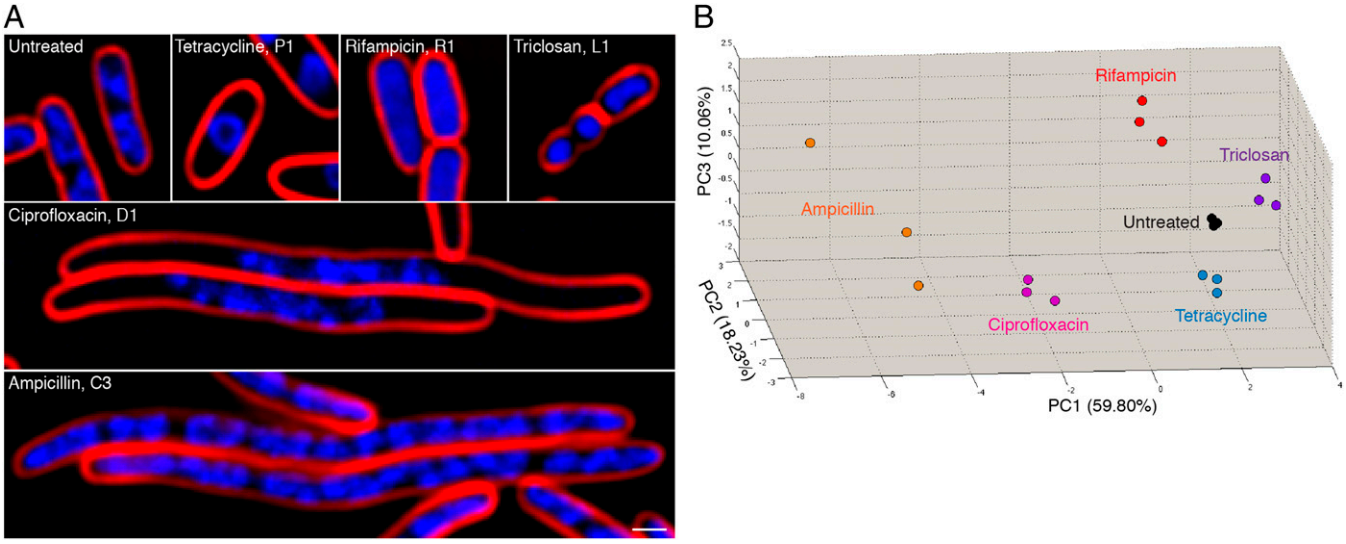

Fig. 1. Bacterial cells treated with inhibitors targeting one of five major biosynthetic pathways (DNA, protein, RNA, peptidoglycan, lipid) have unique cytological profiles. (*A*) *E. coli* cells were treated with 5x MIC of each antibiotic for 2 h and stained with FM4-64 (red) and DAPI (blue). (Scale bar, 1 μm.) (*B*) A 3D PCA graph using PC1 (59.80%), PC2 (18.23%), and PC3 (10.06%). Variables that contribute to each principal component (PC) are summarized in Fig. S1. Each antibiotic is color coded with three replicates shown. Three independent cultures of bacteria were treated with each antibiotic, and cell morphologies were measured as described in *Materials and Methods*.

Results

Categorizing Inhibitors of Five Major Biosynthetic Pathways. We first sought to determine whether BCP can distinguish between inhibitors of the five major pathways assayed by MMS (translation, transcription, DNA replication, lipid synthesis, and peptidoglycan synthesis). In Fig. 1*A*, we show cells that have been treated for 2 h with one inhibitor from each class (tetracycline, rifampicin, ciprofloxacin, triclosan, and ampicillin) at 5× the minimal inhibitory concentration (MIC). Cells in each category had strikingly different morphologies, demonstrating that compounds targeting different pathways generated unique cytological profiles. Notable among these is tetracycline, which produced toroidal chromosomes in wide cells, and rifampicin, which produced decondensed chromosomes in wide cells. To quantitatively analyze these results, we performed the experiments in triplicate, measured cell morphologies resulting from treatment with each antibiotic (Tables S2 and S3), and performed principal component analysis (PCA) to categorize cells with similar morphologies. As shown in Fig. 1*B* and Fig. S1, each of the five categories of antibiotics was quantitatively separated from each other

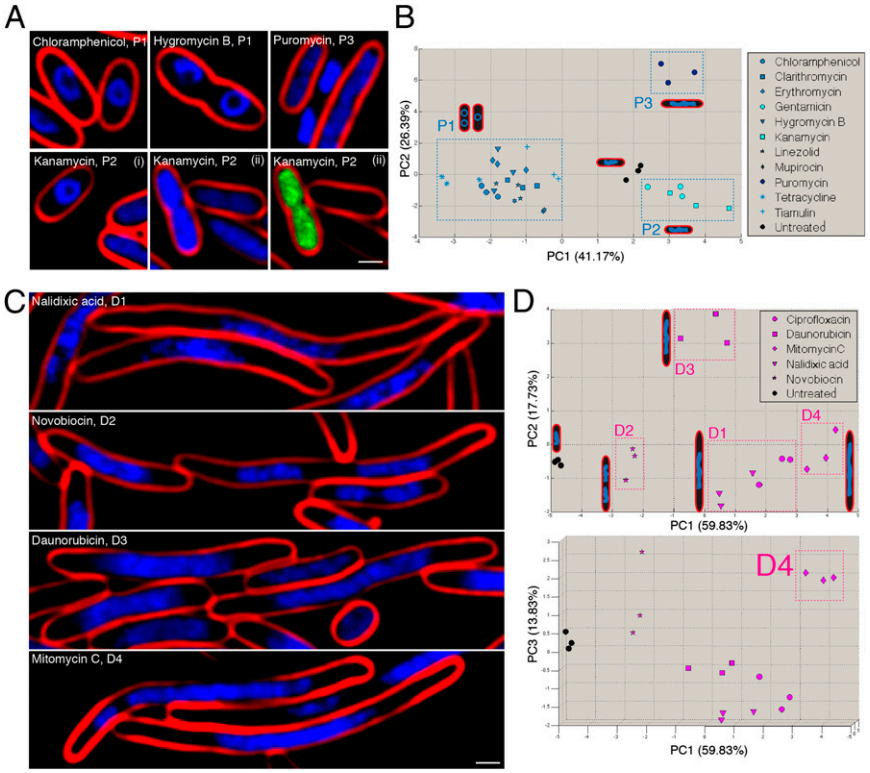

Fig. 2. Cytological profiling of translation and DNA replication inhibitors. (*A* and *B*) Images of cells treated with protein translation inhibitors (*A*) were used to construct profiles that divided them into three subclasses (P1–P3) (*B*). (*C* and *D*) DNA replication inhibitors formed four subclasses (D1–D4). Subclass D4 is distinguishable from D1 by plotting PC1 versus PC3 (*D*, *Lower* graph). The boundaries of the subgroups (boxes) were determined empirically from the training set using compounds with known mechanisms of action and the Euclidean distance cluster map shown in Figs. S2*E* and S3*D*. In all images, cell membranes are stained with FM4-64 (red), DAPI (blue), and SYTOX green (green). SYTOX green brightly stains only cells with permeabilized membranes and is absent from most images. (*A*) Kanamycin generates two types of profiles in a mixed population. Therefore, two fields are shown. *Left* shows altered DNA morphology (*i*), the *Right* two panels (*ii*) show the same field of cells with altered membrane permeability (*ii*, *Center*, FM4-64 and DAPI; *ii*, *Right*, FM4-64 and SYTOX green). (Scale bar, 1 μm.) Details of PCA graphs *B* and *D* are provided in Figs. S2 and S3, respectively.

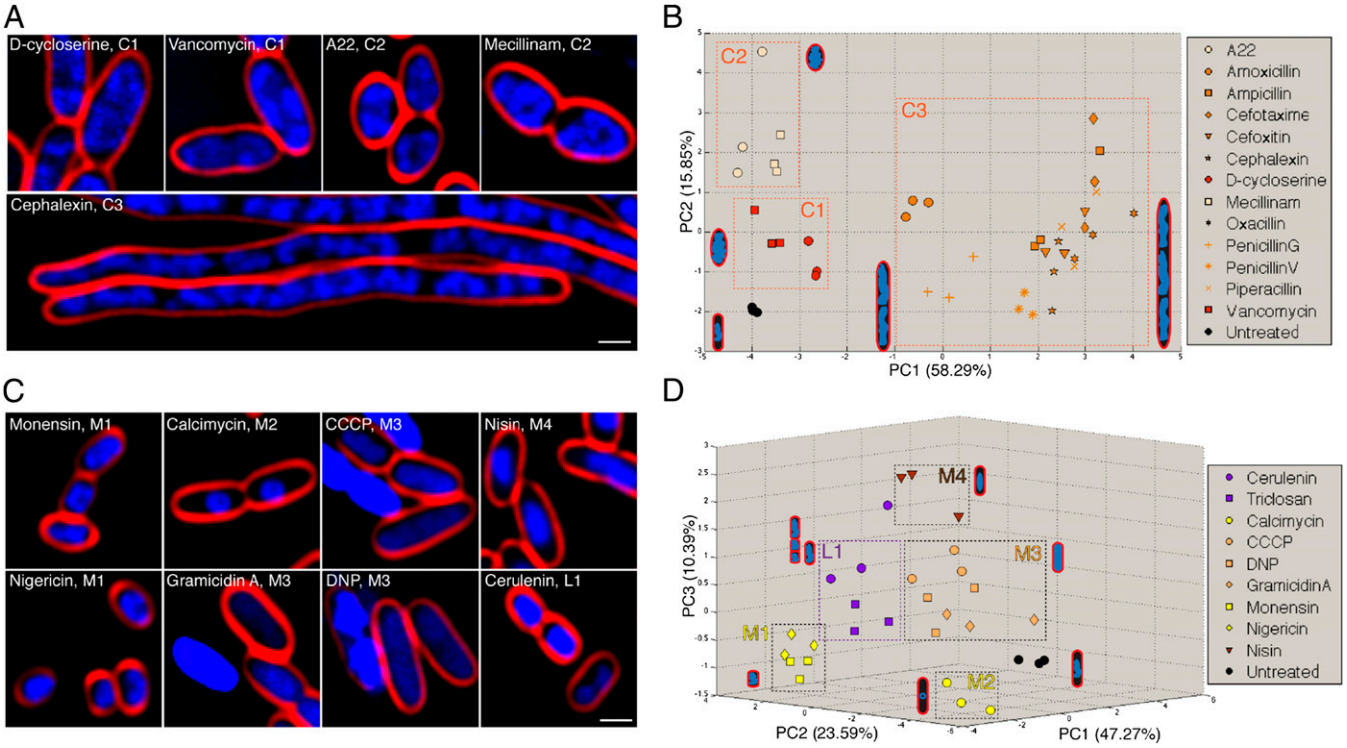

Fig. 3. Cytological profiling of cell-wall and lipid biosynthesis inhibitors. (*A* and *C*) Bacterial cells were treated with each cell-wall synthesis inhibitor (*A*), lipid biosynthesis inhibitor (*C*), and membrane active compounds (*C*), stained with FM4-64 (red) and DAPI (blue). (Scale bars, 1 μm.) (*B*) PCA graph showing PC1 (58.29%) and PC2 (15.85%), using unweighted variables from the cell-wall synthesis inhibitors, which form three subclasses (C1–C3). (*D*) A 3D PCA graph, PC1 (47.27%) and PC2 (23.59%) and PC3 (10.39%), using unweighted variables from membrane active compounds and lipid biosynthesis inhibitors. Variables contributing to each PC are summarized in Figs. S4 and S5. The boundaries of the subgroups (boxes) were determined empirically from the training set using compounds with known MOA and the Euclidean distance cluster map shown in Figs. S4*E* and S5*D*.

and replicates clustered closely together, demonstrating that cytological profiles for these compounds were reproducible. Thus, BCP can rapidly and quantitatively discriminate between the five major classes of antibiotics assayed by MMS.

Detection of Inhibitor Subclasses by BCP. To determine whether cytological profiles were conserved across different mechanistic classes of protein-synthesis inhibitors, we examined eleven different inhibitors belonging to eight structural classes that have a variety of biochemical effects on the ribosome. We found that we could clearly distinguish three subclasses of protein-synthesis inhibitors that have distinct biochemical mechanisms of action (Fig. 2 *A* and *B* and Fig. S2). Subclass P1 inhibitors, which are defined from the training set as box P1 in Fig. 2*B* and Fig. S2*E*, completely block peptide elongation [e.g., tetracycline (Fig. 1*A*) and chloramphenicol (Fig. 2*A*)] and produce toroid-shaped chromosomes and wide cells. Subclass P2 inhibitors, which include most of the aminoglycosides, are thought to both promote mistranslation and effect membrane permeability (21). In keeping with these two proposed MOA, each subclass P2 inhibitor produced two distinct cell populations: (*i*) those with altered chromosome morphology and (*ii*) those with altered membrane permeability (Fig. 2*A*). The one notable exception was the aminoglycoside hygromycin B, which inhibits chain elongation (22) and falls in subclass P1. The subclass P3 inhibitor puromycin causes premature chain termination and formed a distinct category on the PCA plot (Fig. 2*B*). Thus, BCP can discriminate between molecules that have a similar structure but different effects on translation. It can also cluster molecules that have different structures but the same MOA and identify individual molecules (such as the aminoglycosides) that have more than one MOA.

Inhibitors of DNA gyrase, topoisomerase II, DNA intercalating agents, and DNA cross-linking agents fall into a single group as DNA replication inhibitors in MMS assays (10, 23, 24). To determine whether BCP could provide more detailed information on DNA synthesis inhibitors, we profiled five compounds belonging to four structural classes that interact with different cellular targets. We found that BCP could identify four subclasses that correlated with their MOA (Fig. 2 *C* and *D* and Fig. S3). Compounds that primarily target the GyrA subunit of DNA gyrase (ciprofloxacin, nalidixic acid) generated a reproducibly distinct profile (D1) from novobiocin (D2), which targets the GyrB subunit. The intercalating agent daunorubicin (D3) and the DNA cross-linker mitomycin C (D4) also formed separate subclasses. These groups have related profiles that can be distinguished by using three principal components in the analysis (e.g., D4 versus D1–D3, Fig. 2*D*, *Lower* and Fig. S3*D*).

We next profiled a variety of cell-wall synthesis inhibitors, membrane-active compounds, lipid-biosynthesis inhibitors (Fig. 3 and Figs. S4 and S5), and transcription and nucleotide-synthesis inhibitors (Fig. S6). We found that all tested antibiotics targeting different cellular pathways generated reproducibly distinct profiles. Cell-wall synthesis inhibitors fell into three different groups (Fig. 3 *A* and *B*) depending on whether they inhibit the availability of peptidoglycan precursors (C1), inhibit lateral cell-wall synthesis either by preferentially inhibiting PBP2 or by inhibiting MreB (C2), or whether they target PBP3 involved in cell division (C3).

Compounds that interfere with membrane bioenergetics (Fig. 3 *C* and *D* and Fig. S5) fell into four distinct categories based on their MOA, including the monovalent and divalent cation shuttles (M1 and M2, respectively), proton gradient dissipators (M3), and a pore-forming molecule (M4). These four categories were also distinct from inhibitors of lipid biosynthesis (L1). The profiles generated by the RNA transcription inhibitors actinomycin D and rifampicin were also distinct from other classes of antibiotics and formed two subclasses (R1 and R2, Fig. S6).

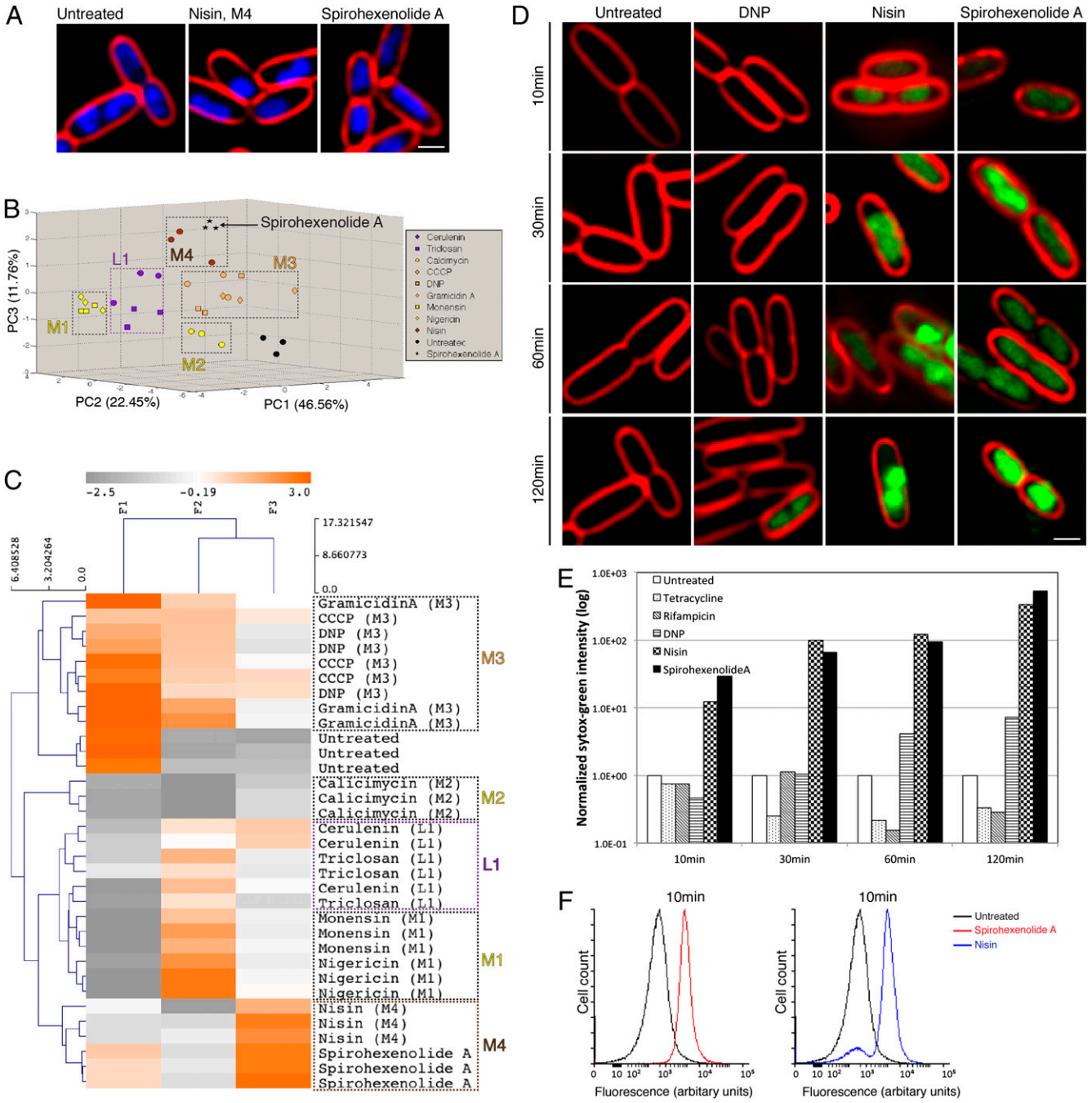

Fig. 4. Spirohexenolide A MOA determination by BCP. (*A*) Bacterial cells treated with spirohexenolide A and nisin were stained with FM 4–64 (red) and DAPI (blue). (*B* and *C*) Cells treated with spirohexenolide A clustered with nisin (M4). (*B*) A 3D PCA graph, PC1 (46.56%) and PC2 (22.45%) and PC3 (11.76%), using unweighted variables from membrane active compounds, lipid biosynthesis inhibitors, and spirohexenolide A. (*C*) Cluster map of spirohexenolide A, using PC1, PC2, and PC3 values from the PCA. (*D*) Bacterial cells treated with an energy poisoning agent DNP, a pore-forming molecule nisin, and spirohexenolide A for various times, stained with FM 4–64 (red) and SYTOX Green (green). SYTOX Green intensity was normalized to the brightest sample. (*E*) A graph of the normalized average SYTOX Green intensity per pixel of cells treated with each antibiotic for 10, 30, 60, and 120 min. Approximately 1,000 cells total were measured. (*F*) PMF assay using DiBAC4(5) stained *E. coli*. Cells were treated for 10 min with spirohexenolide A (red) or nisin (blue) and subjected to flow cytometry. A total of 10,000 cells were counted.

Our results demonstrate that all compounds that target different cellular pathways generate quantitatively distinct cytological profiles. To determine whether we could use these profiles to identify the cellular pathways targeted by a collection of antibiotics, we performed a double-blind BCP experiment. A total of 18 different known compounds were blinded and placed into three separate groups of 10, and then each group was separately profiled against *Esherichia coli.* Based solely on the cytological profile generated after drug exposure, we were able to correctly assign all 30 independently tested compounds to the correct cellular target (Table S4). This test confirmed our conclusion that bacterial cytological profiling is a rapid and powerful approach for determining the cellular pathway targeted by molecules even when their molecular identities are unknown.

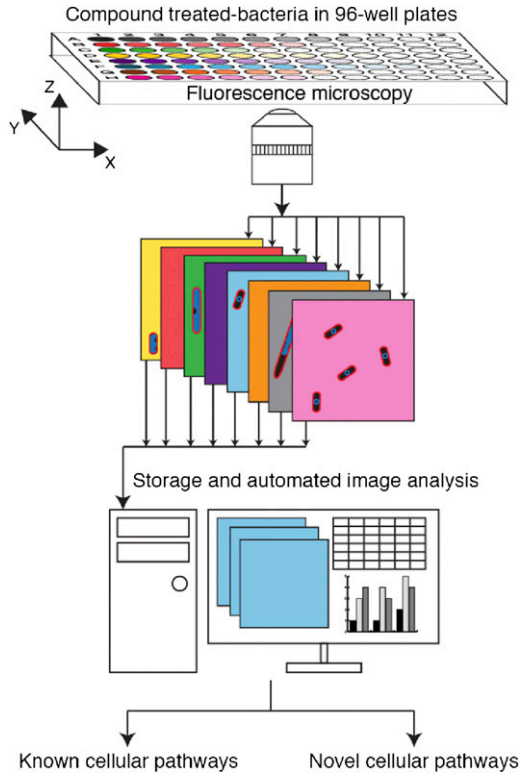

Fig. 5. Bacterial cytological profiling high-throughput screening (BCP-HTS). Bacterial cultures are grown in 96-well plates in the presence of different concentrations of antibacterial molecules. At specified time points, treated cultures are transferred to a microscopic 96-well plate, and images are collected using a fluorescence microscope. All stored images can be analyzed in batch using automated image analysis software and compared with an existing profile database to identify the target. Compounds with completely unique cellular targets will form distinct categories that will be high priority for further analysis. The power of the analysis increases over time as more molecules with known mechanisms of action are characterized.

Identifying the Mode of Action of Spirohexenolide A. We next used BCP to provide information on the MOA of spirohexenolide A (Fig. S7*A*) (25), a spirotetronate natural product with a previously unknown MOA that kills mammalian cells, Gram positive bacteria, including MRSA, as well as the *E. coli lptD4213* mutant (26). Although spirohexenolide A was recently reported to inhibit human macrophage migration inhibitor factor (hMIF), it likely has a different target in bacterial cells because bacteria do not contain hMIF (27). Spirohexenolide A-treated cells had an overall profile identical to nisin-treated cells (Fig. 4 *A*–*C* and Fig. S7), suggesting that spirohexenolide A has an MOA similar to nisin. Nisin binds lipid II and rapidly forms pores in the membrane (28) so we tested whether spirohexenolide A compromised membrane integrity using the membrane-impermeable DNA stain SYTOX Green, which cannot enter intact cells. Both nisin- and spirohexenolide A-treated cells showed increased SYTOX Green fluorescence intensity within 10 min of antibiotic exposure (Fig. 4 *D* and *E*), suggesting that spirohexenolide A rapidly permeabilized the cell membrane. Nisin also collapses the proton motive force (PMF) of bacteria (29) so we used the PMF sensitive dye DiBAC4(5) and Fluorescence-Activated Cell Sorting (FACS) to determine whether spirohexenolide A collapses the PMF (20, 30). Immediately upon addition of spirohexenolide A, cells were rapidly permeabilized and showed high fluorescence intensity of the DiBAC4(5) PMF dye, identical to nisin-treated cells (Fig. 4*F*), suggesting that spirohexenolide A rapidly depletes PMF. Thus, spirohexenolide A likely acts by disrupting the cytoplasmic membrane.

Discussion

Cytological profiling in eukaryotic cells relies upon measuring a large number of cytoskeletal markers (18). Because bacteria are 100 times smaller than the typical eukaryotic cell and lack all of the organelles and markers used in those studies, it has long been assumed that cytological profiling could not be applied to bacteria. Here, we show that BCP is a simple, one-step assay that provides an immensely powerful approach for identifying the cellular pathways targeted by molecules, a key step in determining the MOA. BCP has many advantages over other approaches: it is faster, provides higher resolution for identifying more pathways, and can be performed in very small (microliter scale) culture volumes. BCP also does not require a set of specialized strains like many other methods (13–17). Because a single BCP experiment is sufficient to identify the cellular pathway targeted, the BCP workflow is simple and can be performed in high throughput. BCP can therefore be used for primary screening of compounds to identify molecules that target specific cellular pathways without the need for slow and labor-intensive analysis. Because one can easily monitor changes in cell morphology after exposure to various concentrations of different molecules (Fig. 5), BCP high-throughput screening (BCP-HTS) does not require growth inhibition data, such as MIC or viable cell counts, before screening. This advantage makes the method suitable for primary whole-cell screening of newly made libraries. The power of interpreting cytological profiles increases over time as more molecules with known mechanisms of action are characterized. When compounds with completely unique cellular targets are profiled, they will form unique categories and might be given high priority for further analysis. Because bacteria have evolved resistance to nearly all known antibiotics, identifying molecules with different mechanisms of action is of high priority.

One limitation of BCP is that it does not identify the precise molecular target and is therefore complementary to approaches such as isolating resistant mutants or screening a large collection of sensitized strains. In addition, newly isolated compounds that represent the first known inhibitors of a pathway will require additional experimental methods to determine and validate their targets.

Why does BCP work? A bacterial cell is built by thousands of enzymes working in unison. We speculate that the various pathways are largely uncoupled by checkpoints so inactivating a single essential enzyme reduces one key product, while the rest of the cell continues to replicate, leading to unique cell-shape changes in response to each specific challenge. In nearly all cases, the cytological profiles produced in response to antibiotics can be explained in terms of their physiological effects. For example, compounds that block translation lead to chromosome compaction due to the interference with coordinated translation and insertion of proteins into the membrane (31, 32) whereas compounds that block transcription lead to chromosome decondensation due to the absence of active RNA polymerase (33). BCP takes advantage of the paucity of cell-cycle checkpoints in bacteria and the advent of high-resolution imaging to allow the rapid identification of the cell pathway affected by thousands of compounds, eliminating a longstanding bottleneck in academic programs and in antibiotic discovery programs. BCP can be applied to a wide range of studies that involve compounds that kill bacteria, including studies of the innate immune system, complex microbial communities, evolution of antibiotics and mechanisms of resistance, as well as efforts to find antibiotics that are active against multidrug resistant bacteria.

Materials and Methods

Strain and Antibiotics. *E. coli lptD4213* was used in this study (26). Forty-one antibiotics were used that include 26 structural classes of antibiotics used in the clinic (Table S1). Solutions of antibiotics in Table S1 were prepared using the recommended concentrations and solvents from the manufacturers.

Minimal Inhibitory Concentration Determination. Minimal inhibitory concentration (MIC) data shown in Table S1 were determined by the microdilution

MICROBIOLOGY

method (34). Overnight cultures of *E. coli* were diluted 1:100 into LB medium and grown at 30 °C to an OD_{600} of 0.2 (early exponential phase). Exponential-phase cell cultures were diluted 1:100 into the LB medium containing different concentrations of each antibiotic in a 96-well plate. MIC was obtained after an overnight incubation at 30 °C.

Fluorescence Microscopy. Exponential-phase cell cultures were treated with 5x MIC and grown in a roller at 30 °C. Treated cultures were harvested after 2 h and stained with 1 $\mu g \cdot mL^{-1}$ FM4-64 (35), 2 $\mu g \cdot mL^{-1}$ DAPI, and 0.5 μM SYTOX-Green (Molecular Probes/Invitrogen). Cultures were then centrifuged at 3,300 × *g* for 30 s in a microcentrifuge and resuspended in 1/10 volume of the original cultures. Three microliters of concentrated cells were transferred onto an agarose pad containing 1.2% agarose and 20% LB medium for microscopy. Microscopy was performed as previously described (20). Exposure time of each wavelength was the same throughout every experiment included in the statistical analysis of all training sets of antibiotics.

Cytological Profiling. Cell morphology was measured by the ImageJ v1.46 according to the analyze tool parameters. Briefly, polygons were drawn on an experimental field using membrane or nucleoid as a guide to measure area (μm^2), perimeter (μm), length (μm), width (μm), and circularity of both membrane and nucleoid. Performing on nondeconvolved images, average DAPI and SYTOX Green intensity per pixel was determined using the membrane outline, and then subtracted by its own background intensity. Finally, DAPI and SYTOX Green intensity of treated cells was normalized by untreated cells intensity of the same set of experiments, making intensity data from different experimental sets comparable. Decondensation of the nucleoid was defined by the ratio of corrected nucleoid area and membrane area.

Statistical Analysis. Cell-morphology parameters in Tables S2 and S3 from each antibiotic were obtained from three or more independent experiments. The deviation shown in Tables S2 and S3 represents the SEM. Profiling data were obtained from, if possible, every cell in the imaging fields ($n > 30$ for the elongated cell phenotype, $n > 50$ for the others). Variables reduction was performed using a Principal Component Analysis (PCA) from the XLSTAT (version 2012.5.01) program on Microsoft Excel for Mac 2011 (version 14.1.0). Spearman's rank correlation and unweighted variables were used in PCA. Clustering of each subclass was performed using the Euclidean distance (average linkage) method on MultiExperiment Viewer (v4.7.3). The boundaries of the subgroups (boxes) drawn on the PCA graphs were determined empirically from the training set using compounds with known MOA and a Euclidean distance cluster map.

Double-Blind Tests. Eighteen antibiotics targeting different pathways and two controls (water and DMSO) were included in a double-blinded BCP experiment. Samples were divided into three sets containing 10 compounds in each set and relabeled as A1–A10, B1–B10, and C1–C10. Both the tester and the administrator were not aware of what compound belonged to which subclass of antibiotic, and each set was tested independently.

Flow Cytometry. Analysis of the *E. coli* proton motive force (PMF) by flow cytometry was carried out as described in ref. 20. Cell cultures were treated with spirohexenolide A or nisin at 30 °C for 10 min.

ACKNOWLEDGMENTS. We thank A. Derman, A. Lamsa, D. Quach, and A. Desai for technical assistance in this project. P.N. was supported by a Royal Thai Government Science and Technology Scholarship. This study was supported by National Institutes of Health Grants GM1R073898 and AI095125.

1. Hooper LV, Littman DR, Macpherson AJ (2012) Interactions between the microbiota and the immune system. *Science* 336(6086):1268–1273.
2. Hill DA, Artis D (2010) Intestinal bacteria and the regulation of immune cell homeostasis. *Annu Rev Immunol* 28:623–667.
3. Ley RE, Peterson DA, Gordon JI (2006) Ecological and evolutionary forces shaping microbial diversity in the human intestine. *Cell* 124(4):837–848.
4. Tremaroli V, Bäckhed F (2012) Functional interactions between the gut microbiota and host metabolism. *Nature* 489(7415):242–249.
5. Romero D, Traxler MF, López D, Kolter R (2011) Antibiotics as signal molecules. *Chem Rev* 111(9):5492–5505.
6. Zasloff M (2002) Antimicrobial peptides of multicellular organisms. *Nature* 415(6870): 389–395.
7. Nikaido H (2009) Multidrug resistance in bacteria. *Annu Rev Biochem* 78:119–146.
8. Silver LL (2011) Challenges of antibacterial discovery. *Clin Microbiol Rev* 24(1):71–109.
9. Payne DJ, Gwynn MN, Holmes DJ, Pompliano DL (2007) Drugs for bad bugs: Confronting the challenges of antibacterial discovery. *Nat Rev Drug Discov* 6(1):29–40.
10. Cotsonas King A, Wu L (2009) Macromolecular synthesis and membrane perturbation assays for mechanisms of action studies of antimicrobial agents. *Current Protocols in Pharmacology*, eds Enna SJ, et al. (Wiley, Hoboken, NJ).
11. Bandow JE, Hecker M (2007) Proteomic profiling of cellular stresses in *Bacillus subtilis* reveals cellular networks and assists in elucidating antibiotic mechanisms of action. *Systems Biological Approaches in Infectious Diseases*, eds Boshoff HI, Barry CE (Birkhäueser, Basel, Switzerland), pp 79–101.
12. Donald RGK, et al. (2009) A *Staphylococcus aureus* fitness test platform for mechanism-based profiling of antibacterial compounds. *Chem Biol* 16(8):826–836.
13. Freiberg C, Fischer HP, Brunner NA (2005) Discovering the mechanism of action of novel antibacterial agents through transcriptional profiling of conditional mutants. *Antimicrob Agents Chemother* 49(2):749–759.
14. Xu HH, Real L, Bailey MW (2006) An array of *Escherichia coli* clones over-expressing essential proteins: A new strategy of identifying cellular targets of potent antibacterial compounds. *Biochem Biophys Res Commun* 349(4):1250–1257.
15. Nichols RJ, et al. (2011) Phenotypic landscape of a bacterial cell. *Cell* 144(1):143–156.
16. Singh SB, Phillips JW, Wang J (2007) Highly sensitive target-based whole-cell antibacterial discovery strategy by antisense RNA silencing. *Curr Opin Drug Discov Devel* 10(2):160–166.
17. Li X, et al. (2004) Multicopy suppressors for novel antibacterial compounds reveal targets and drug efflux susceptibility. *Chem Biol* 11(10):1423–1430.
18. Mitchison TJ (2005) Small-molecule screening and profiling by using automated microscopy. *ChemBioChem* 6(1):33–39.
19. Mayer TU, et al. (1999) Small molecule inhibitor of mitotic spindle bipolarity identified in a phenotype-based screen. *Science* 286(5441):971–974.
20. Lamsa A, Liu WT, Dorrestein PC, Pogliano K (2012) The *Bacillus subtilis* cannibalism toxin SDP collapses the proton motive force and induces autolysis. *Mol Microbiol* 84(3):486–500.
21. Jana S, Deb JK (2006) Molecular understanding of aminoglycoside action and resistance. *Appl Microbiol Biotechnol* 70(2):140–150.
22. Peske F, Savelsbergh A, Katunin VI, Rodnina MV, Wintermeyer W (2004) Conformational changes of the small ribosomal subunit during elongation factor G-dependent tRNA-mRNA translocation. *J Mol Biol* 343(5):1183–1194.
23. Guan L, Blumenthal RM, Burnham JC (1992) Analysis of macromolecular biosynthesis to define the quinolone-induced postantibiotic effect in *Escherichia coli*. *Antimicrob Agents Chemother* 36(10):2118–2124.
24. Menzel TM, et al. (2011) Mode-of-action studies of the novel bisquaternary bisnaphthalimide MT02 against *Staphylococcus aureus*. *Antimicrob Agents Chemother* 55(1):311–320.
25. Kang MJ, et al. (2009) Isolation, structure elucidation, and antitumor activity of spirohexenolides A and B. *J Org Chem* 74(23):9054–9061.
26. Ruiz N, Falcone B, Kahne D, Silhavy TJ (2005) Chemical conditionality: A genetic strategy to probe organelle assembly. *Cell* 121(2):307–317.
27. Yu W-L, et al. (2013) Spirohexenolide A targets human macrophage migration inhibitory factor (hMIF). *J Nat Prod* 76(5):817–823.
28. Wiedemann I, et al. (2001) Specific binding of nisin to the peptidoglycan precursor lipid II combines pore formation and inhibition of cell wall biosynthesis for potent antibiotic activity. *J Biol Chem* 276(3):1772–1779.
29. Bruno ME, Kaiser A, Montville TJ (1992) Depletion of proton motive force by nisin in *Listeria monocytogenes* cells. *Appl Environ Microbiol* 58(7):2255–2259.
30. Sims PJ, Waggoner AS, Wang CH, Hoffman JF (1974) Studies on the mechanism by which cyanine dyes measure membrane potential in red blood cells and phosphatidylcholine vesicles. *Biochemistry* 13(16):3315–3330.
31. Cabrera JE, Cagliero C, Quan S, Squires CL, Jin DJ (2009) Active transcription of rRNA operons condenses the nucleoid in *Escherichia coli*: Examining the effect of transcription on nucleoid structure in the absence of transertion. *J Bacteriol* 191(13): 4180–4185.
32. Hud NV, Downing KH (2001) Cryoelectron microscopy of λ phage DNA condensates in vitreous ice: The fine structure of DNA toroids. *Proc Natl Acad Sci USA* 98(26): 14925–14930.
33. Jin DJ, Cabrera JE (2006) Coupling the distribution of RNA polymerase to global gene regulation and the dynamic structure of the bacterial nucleoid in *Escherichia coli*. *J Struct Biol* 156(2):284–291.
34. Matthew AW (2006) Methods for Dilution Antimicrobial Susceptibility Tests for Bacteria That Grow Aerobically; Approved Standard. Seventh Edition (CLSI, Wayne, PA), pp 14–18.
35. Pogliano J, et al. (1999) A vital stain for studying membrane dynamics in bacteria: a novel mechanism controlling septation during *Bacillus subtilis* sporulation. *Mol Microbiol* 31(4):1149–1159.